



## Sinkhole monitoring and early warning: An experimental and successful GB-InSAR application



Emanuele Intrieri\*, Giovanni Gigli, Massimiliano Nocentini, Luca Lombardi, Francesco Mugnai, Francesco Fidolini, Nicola Casagli

Università degli Studi di Firenze, Earth Science Department, via La Pira 4, 50121 Firenze, Italy

### ARTICLE INFO

#### Article history:

Received 26 September 2014

Received in revised form 15 April 2015

Accepted 17 April 2015

Available online 25 April 2015

#### Keywords:

Sinkhole

Early warning

Radar interferometry

Karst

### ABSTRACT

Sinkholes represent a natural risk that may hit catastrophically without clearly detectable precursors. However, they are often overlooked by people and administrators. Therefore sinkhole monitoring and associated early warnings constitute important research topics but, currently, only a few papers about sinkhole prediction can be found. In this paper an experience of sinkhole monitoring and early warning with GB-InSAR is described. The latter is a highly precise instrument that is able to produce displacement maps with metric spatial resolution. The described activities were carried out on Elba Island (central Italy), where karstified limestone set off the occurrence of nine sinkholes since 2008, all within less than 3000 m<sup>2</sup>, causing major damage to an important road and many indirect losses. In 1 year of monitoring two deforming areas were detected, and the point where a sinkhole was about to propagate to the street level was predicted, thus permitting the preventive closure of the road. The deformation area was larger than the hole generated by the sinkhole, thus showing a subsidence that continued for a prolonged time even after the cavity was filled up. The occurrence of a 1.5-m-wide sinkhole, undetected by the GB-InSAR, also showed the lower detection limit of the instrument.

© 2015 The Authors. Published by Elsevier B.V. This is an open access article under the CC BY-NC-ND license (<http://creativecommons.org/licenses/by-nc-nd/4.0/>).

### 1. Introduction

Sinkhole is a term first introduced by Fairbridge (1968) to define subcircular surface depressions or collapse structures formed by the collapse of small subterranean karst cavities. With time this definition has been broadened and this word is now often used to describe surface depressions regardless of their shape and of their karstic, anthropic, deep pipings, or mixed genesis (Kaufmann and Quinif, 1999; Brinkmann et al., 2008; Caramanna et al., 2008; Guarino and Nisio, 2012; Krawczyk et al., 2012). Sometimes it is also used as a synonym of doline (Williams, 2003; Waltham et al., 2005).

Many types of sinkholes can be individuated depending on the processes that guide their formation, and the scientific literature is populated by a large variety of different classifications based on genesis criteria (Cramer, 1941; Beck and Sinclair, 1986; White, 1988; Williams, 2003; Waltham et al., 2005; Gutiérrez and Guerrero, 2008).

Because sinkholes originate above karstified rocks or, in general, subterranean cavities, commonly they are densely clustered in certain regions (sinkhole prone areas), while they are completely absent in others. For example in the 7-km<sup>2</sup>-wide area of San Vittorino's Plain (central Italy), the presence of at least 35 sinkholes has been recognized (Tassi et al., 2012); in Tampa, Florida (442 km<sup>2</sup>), Brinkmann et al. (2008)

identified 293 sinkholes; in the 6-km<sup>2</sup>-wide area studied by Bruno et al. (2008) in the Apulia region (Southern Italy), 58 sinkholes have been mapped.

The most common predisposing factors are the presence of soluble rocks subject to karstic processes, anthropic subterranean cavities, poor geomechanical parameters of the bedrock, and (acidic) groundwater circulation fostering the dissolution of certain rocks. In order for these phenomena to occur, triggering factors are also necessary. These are often related to the circulation of groundwater that generates erosion in the sediments above the layer that includes the cavities. For example, variations in the phreatic level caused by pumping increase the local hydraulic gradient, whereas rainfall produces erosion during infiltration and by feeding subterranean streams. Other triggers include loading (Nisio et al., 2007), earthquakes (Snyder et al., 1989; Ferrel et al., 2004), anthropic vibrations (Parise, 2012), and deep piping processes caused by high pressure fluids rich in CO<sub>2</sub> and H<sub>2</sub>S upwelling along fracture–fault systems (Nisio et al., 2007; Caramanna et al., 2008). In most cases, sinkholes develop from the bottom layer (where the cavity is formed) to the surface (Littlefield et al., 1984; Derbyshire and Mellors, 1988; Faccenna et al., 1993).

Sinkholes can cause severe economic damages, especially in urban areas, and even human life loss, in cases of catastrophic collapse (Bezuidenhout and Enslin, 1970; Vallario, 2001; Galve et al., 2011, and references therein). Losses from sinkholes can be direct losses (which occur during and immediately after the event and include loss of

\* Corresponding author.

E-mail address: [emanuele.intrieri@unifi.it](mailto:emanuele.intrieri@unifi.it) (E. Intrieri).

human life and damage to property), indirect losses (which are more widespread and may involve people or businesses not in the hit area; losses include interruption to business, transportation networks and communications, the costs of assistance, storage and accommodation for those displaced by the phenomenon), and intangible losses (which are more difficult to quantify in monetary terms and include detours or tail-backs on the journey to work, psychological impairments, and the cost of delocalization from an area at risk).

For instance in Pasco County (Florida), Citizens Property Insurance paid more than \$17 million in 2004 owing to sinkholes (Therolf, 2005), while in the city of Calatayud (Spain) a single event affecting buildings caused 4.8 million € of direct economic losses (Gutiérrez et al., 2004).

Effective monitoring and early warning systems are needed to be able to forecast sinkhole collapses and thus reduce the risk for people and property.

The main issue is related to the quick identification of deformational anomalies, which are generally very small with respect to the sinkhole-prone area. Moreover, once an anomaly is observed, we should be able to monitor its behaviour with high accuracy as the precursory movements of a main collapse are generally very limited.

This paper aims at presenting a monitoring approach which demonstrated to be very effective in early identification and monitoring of sinkholes. The presented experience was also very useful, as it allowed us to deeply investigate the limits and constraints of sinkhole monitoring from logistic-geometric and technical points of view.

## 2. Sinkhole deformation monitoring

Contrary to other fields of geological hazards monitoring, where specific instruments have been developed during the years and are now commonly used, in the case of sinkholes a particular tool developed especially for this purpose is lacking; therefore the techniques usually adopted are derived from other fields, such as landslide monitoring.

The reason for this probably lies in a general lack of *sinkhole culture* in people's awareness and also in the intrinsic difficulties of detecting sinkhole deformations before the collapse. One of these difficulties is caused by the abrupt nature they can manifest, especially in the case of bedrock or caprock collapse, where the involved material is mainly governed by brittle behaviour (Gutiérrez and Guerrero, 2008). On the other hand we may expect that, in the case of cover collapse, measurable plastic deformation may occur days before the failure; we can also speculate that the entity of such deformation, when occurring, should be in the order of a few millimetres to a few centimetres. These expectations seem to be confirmed by the few cases of sinkhole prediction that can be found in the literature (Nof et al., 2013; Jones and Blom, 2014). These authors were able to detect precursor deformations of sinkholes, respectively, through new generation satellite interferometry (Cosmo SkyMed constellation) and through airborne interferometry along the Dead Sea and in Louisiana.

In the case of Camaiore (central Italy), in the night between 14 and 15 October 1995, cracks on buildings and structural deformations occurred 6 h before a 35-m-wide sinkhole caused the destruction of a building and severe damage to another five, for a total damage of 2.2 million € (Buchignani et al., 2004a, 2005, 2008); these precursors permitted the avoidance of any loss of life. Other smaller signs of building instability (microcracks, door offsets) were observed 5 days before the event as alleged consequences of an earthquake that occurred 50 km away; however, to identify such smaller signs as sinkhole precursors is not always easy. Ferretti et al. (2004) reported how the permanent scatterers (PS) technique, performed to European remote sensing (ERS) satellite data, showed incipient deformation localized in the sinkhole area of Camaiore starting from mid-1995. Similarly, in the Dead Sea area, Closson et al. (2005) affirmed that 'subsidence could be an indicator of surfaces that are prone to collapse', after observing the occurrence of seven sinkholes preceded by years of subsidence, monitored through ERS data.

Measuring subsidence deformations in known sinkhole-prone areas gives us precious information for prevention and urban planning but also may produce many false alarms, with all the related problems (Lacasse and Nadim, 2008; Intriери et al., 2013b), as not every subsidence deformation leads to a sinkhole; furthermore, for example, instrumental noise could be wrongly identified as deformation. Moreover, even if the area at risk can be identified, it is not easy to detect and forecast the exact location where a sinkhole will occur, contrary to landslides, which are often bound by clear geomorphological signs. This, together with the average small extension of a sinkhole, means a greater difficulty in setting the monitoring network as it must be able to cover the entire susceptible area.

Most of these problems are not present when performing after-event monitoring as the phenomenon is already clearly visible. The scientific literature shows examples of already-formed sinkholes monitored by means of GPS, laser scanner, and total station (Oldow et al., 2008; Kent and Dunaway, 2013), but is lacking cases of such techniques adopted for sinkhole forecasting and early warning.

## 3. Methodology

In this research, a ground-based interferometric synthetic aperture radar (GB-InSAR) has been experimentally used for sinkhole monitoring and early warning. The working principle of a GB-InSAR is to radiate an area with microwaves and to coherently register the backscattered signal. From a single acquisition a complex matrix of values, called as SAR (synthetic aperture radar) image, is obtained. From the imaginary and the real part of each complex number, the phase and amplitude (related to power intensity) information of the corresponding element of the matrix can be calculated. The phase information is used to compute displacement maps following the base principle of radar interferometry, which is to emit microwaves in two different times and to derive the movement of the backscattering targets based on the phase shift between the echoes of the two signals. The amplitude information can be elaborated as well in order to retrieve power images, which are relative to the intensity of the signal reflected by the scenario.

Since the first experiments (Rudolf et al., 1999; Tarchi et al., 1999), this apparatus has been applied to monitor landslides (Intriери et al., 2012; Del Ventisette et al., 2011; Atzeni et al., 2014; Gigli et al., 2014), volcanoes (Di Traglia et al., 2013, 2014; Intriери et al., 2013a), glaciers (Luzi et al., 2007), buildings and structures (Pieraccini et al., 2000) and archaeological monuments (Tapete et al., 2013). In fact GB-InSAR is best used for monitoring structures, rocks, and metallic surfaces. Vegetated areas are generally characterized by low coherence and power intensity, although this issue can be partially solved by installing metallic reflecting elements (corner reflectors) in points of interest.

The only known application to sinkholes is reported by Buchignani et al. (2004b, 2005), although no deformation occurred during that campaign.

A major limitation of this technique is that it only measures the displacement component parallel to the line of sight (LOS), which for obvious practical issues with ground-based platforms can hardly be vertical with respect to the ground. Therefore the choice of the installation point is critical. The relation between the measured displacement ( $d_m$ ) and the real displacement ( $d_r$ ) is expressed by the following:

$$d_m = d_r \cdot \cos\theta \quad (1)$$

where  $\theta$  is the angle between the line of sight and the real direction of movement, which in this case is also corresponding to the incidence angle with the ground.

This problem is partially compensated by the high precision (submillimetre) of the instrument that allows it to detect the slightest deformations; furthermore, contrary to what sometimes happens with other applications, in this case the real direction of movement (vertical) is a priori known, which permits easy calculation of the total

displacement through geometric arguments. The maximum range distance is limited by the corresponding loss in azimuth resolution, that is the ability to separate two objects perpendicular to the distance between the sensor and the target. In fact the higher the range, the lower the azimuth resolution. This might compromise the correct detection of smaller events; on the other hand the long operative range and the wide field of view of the antennas can grant the capability to monitor large areas.

#### 4. A case study on Elba Island: installation and assumptions

In the eastern part of Elba Island (Livorno Province, central Italy), in the locality known as Il Piano (meaning *The Plain* in Italian), between Rio Marina and Rio nell'Elba municipalities, nine sinkholes occurred between 2008 and 2014 (Fig. 1). These events displayed a circular shape, ranged from ~1.5 to ~8 m in diameter, and were all clustered within a <3000-m<sup>2</sup>-wide area. All the recorded events occurred closer than 150 m from a water pumping station.

From a geological point of view, the rocky substrate of the area is mainly constituted by metamorphosed siltstones (Formazione del Cavo) in the western part and by brecciated dolomitic limestone (Calcare Cavernoso) in the eastern part (Fig. 2). These two rock types, belonging to different tectonic units (Grassera unit and Tuscan unit respectively), are juxtaposed by means of a N–S oriented, W-dipping fault and covered by a 20-m-thick Quaternary alluvium. The latter consists of lenticular bodies of gravel and sand within a tabular sandy mud. From a hydrogeological perspective, the outcropping terrains are quite different: the dolomitic limestone shows high permeability, mainly owing to tectonic fracturing and karst phenomena; its formational name derives directly from this peculiar aspect (Calcare Cavernoso can be translated as *cave limestone*). On the other hand, the permeability of metasiltstone is very low, while the alluvial deposits vary considerably between the coarse- and fine-grained layers. For a detailed lithologic description of the aforementioned formations see Bortolotti et al. (2001).

In the study area two main aquifers can be recognized: a superficial one hosted by the Quaternary alluvium and the main one, of karst origin, hosted by the Calcare Cavernoso. The latter is deeply exploited for industrial, agricultural, and drinking purposes. Owing to the high

secondary permeability of the Calcare Cavernoso and to the sinkholes that have occurred so far, it is likely that the two aquifers are at least partially interlinked, resulting in a water flux from the uppermost to the underlying one. In this framework the more likely origin for the studied sinkholes is related to net erosion of sediment from the alluvium caused by downward water circulation between the aquifers. Deep piping phenomena, which are widely reported for similar geological settings (e.g., Salvati and Sasowsky, 2002; Tassi et al., 2012), can be excluded as no gas vents are reported for the study area.

The main elements at risk in this area are represented by a few houses in the Togliatti village and the Provincial road connecting Rio Marina to Rio nell'Elba (PR 26C) (Fig. 1), which is a relevant communication route as it is the only link between Rio Marina (important also for its port that is especially used in tourist seasons) and the rest of the island. Commercial activities (such as a supermarket and an industrial laundry) are also present. Some wells used for providing drinking water are present in this area (Fig. 1).

All the sinkholes detected since 2008 were located above the Calcare Cavernoso Formation and on the PR 26C or very close to it. Where the road crosses different formations no sinkholes have been recorded either from surveys, aerial photos, or witnesses. On the other hand, in the areas upon the karstified limestone covered by crops, other events may have occurred and have yet to be detected or have been concealed by agricultural activity.

Given this worrying situation, the Livorno Province appointed the Department of Earth Science of the University of Florence to set up a monitoring and early warning system for sinkhole hazards. On 19 June 2013 a GB-InSAR operating in Ku band was installed, and it is continuing the monitoring since.

In order to have a LOS as vertical as possible, the GB-InSAR has been placed on a near relief at 420 m from the farthest documented sinkhole (yellow triangle in Figs. 1 and 3). From this point and assuming a vertical direction of movement, the radar has an average angle of ~10° with the ground on the area most interested by sinkholes, meaning that it measures values corresponding to ~20% of a vertical movement.

The resulting radar images cover an area of 64 ha (13 ha of which are characterized by high coherence) entirely comprising the zone affected by sinkholes with an average spatial resolution of 1 m × 1 m (Fig. 4). In this application buildings and streets are characterized by coherence

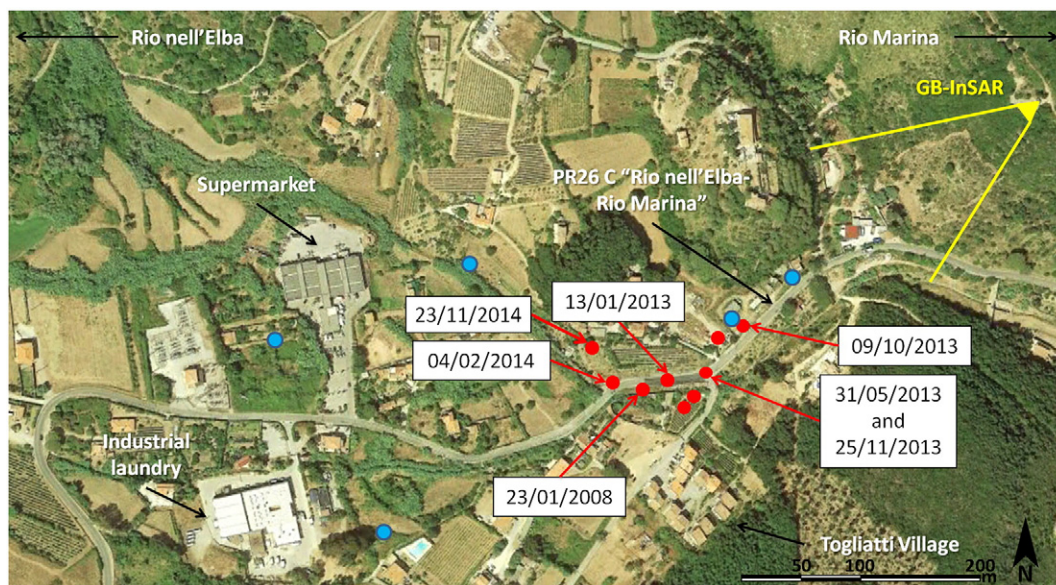


**Fig. 1.** Location of the sinkholes at Il Piano between 2008 and 2014 (red dots). When known, the date of the collapse is also indicated. The 4 February 2014 sinkhole was detected before its collapse (see further in the text), therefore the date of its detection is reported. The blue dots indicate the wells providing drinking water. The yellow triangle represents the GB-InSAR location and its field of view. The main elements at risk are also shown.



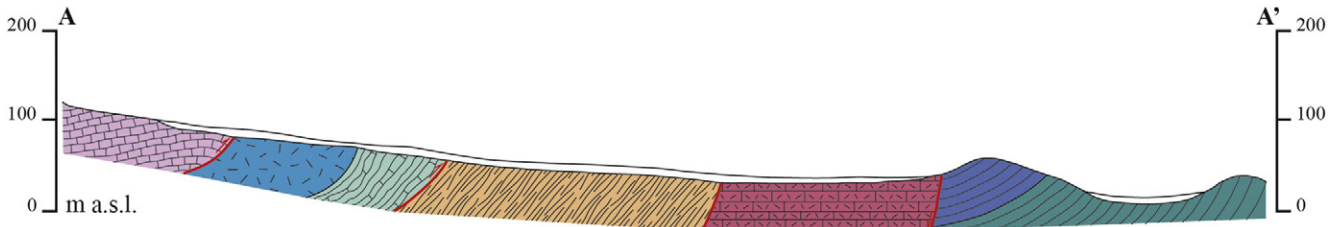
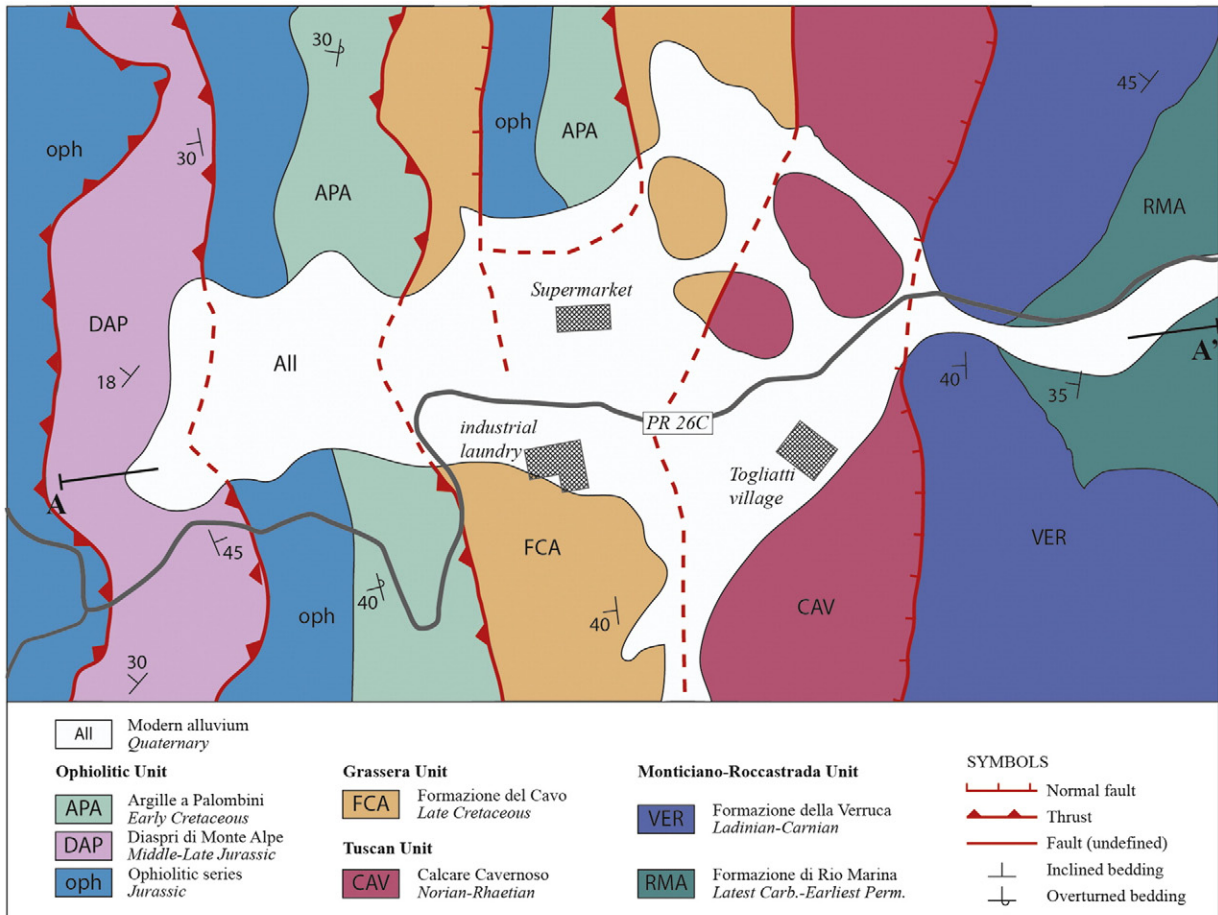


**Fig. 2.** Geological sketch of Il Piano locality and related section. Modified after Bortolotti et al. (2001).

values higher than 0.9 over 24 h and stay high even over longer times; on the other hand the surrounding vegetated zones have an average coherence of 0.7 that dramatically decreases when longer time intervals are considered. Therefore all the analyses are based on 24-hour interferograms from which cumulated data are then obtained. Even with this expedient, data relative to vegetated areas are considered with more caution.

Atmospheric noise is an issue affecting the reliability of any interferometric datum; this has been addressed by correcting the interferograms over a calibration region considered stable. If this assumption is valid, all the displacement recorded in this area is only from atmospheric noise. Because this effect depends on distance, the calibration region has been selected as an elongated area crossing several range distances, so that the pixels of unstable points can be corrected upon the nearest pixels of the correction region.

Little is known about how much possible precursor deformations could predate the occurrence of a catastrophic collapse (Paine et al., 2013), and a few positive experiences only recently have added more information to this issue (Nof et al., 2013; Jones and Blom, 2014). The

hypothesis here is that the tar layer on the street (which represents the major element at risk) can behave like a plastic membrane and experience a deformation detectable by the GB-InSAR before it catastrophically fails.

### 5. Monitoring data

Given the impossibility to predict the exact location of sinkholes (because of their relatively limited spatial extension), the observation of GB-InSAR monitoring data mainly consists in daily accurate visual inspections of interferograms and cumulated displacement maps. Should an anomaly be observed, time series relative to the unstable area are extracted in order to monitor its behaviour through time.

On 9 October 2013 a small sinkhole (just 1.5 m in diameter) occurred at the side of the PR 26C (Figs. 1 and 5A). To precisely locate this point in the GB-InSAR displacement maps, after the event, a corner reflector has been positioned in correspondence to the depression; the corner reflector was visible in the power images and this permitted us to precisely locate the pixel corresponding to the sinkhole area. Then

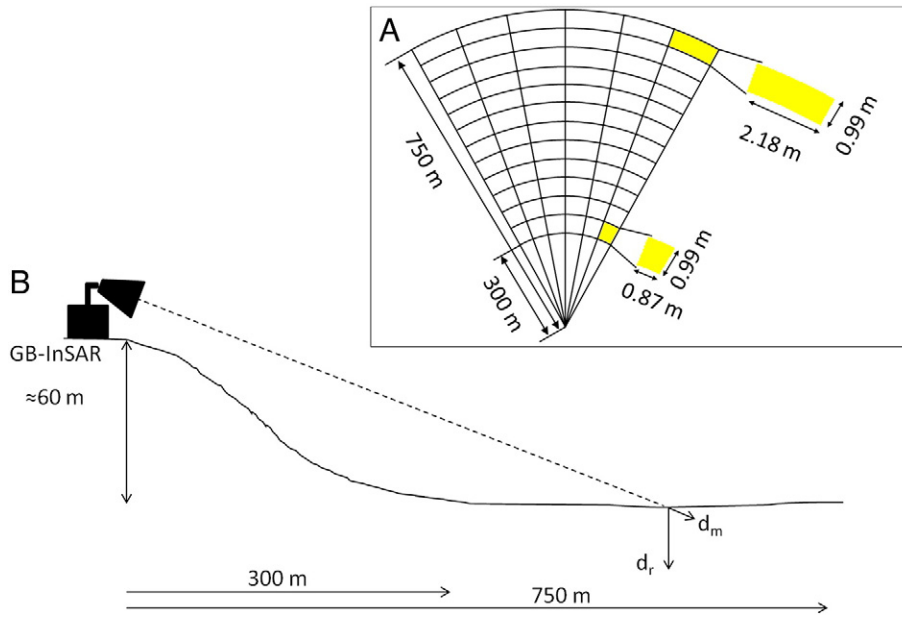


Fig. 3. Schematic representation of the acquisition geometry of the GB-InSAR installed at the Il Piano locality.

a back-analysis of the displacement maps and time series was carried out; however, no deformation was detected. Fig. 5B shows an interferogram relative to the 8–9 October 2013 time span. The red pixels indicate

the absence of movement; pixels of different colours are also visible all over a large area and are owing to noise; in fact, the circled area does not show any difference with respect to the surroundings. This is probably

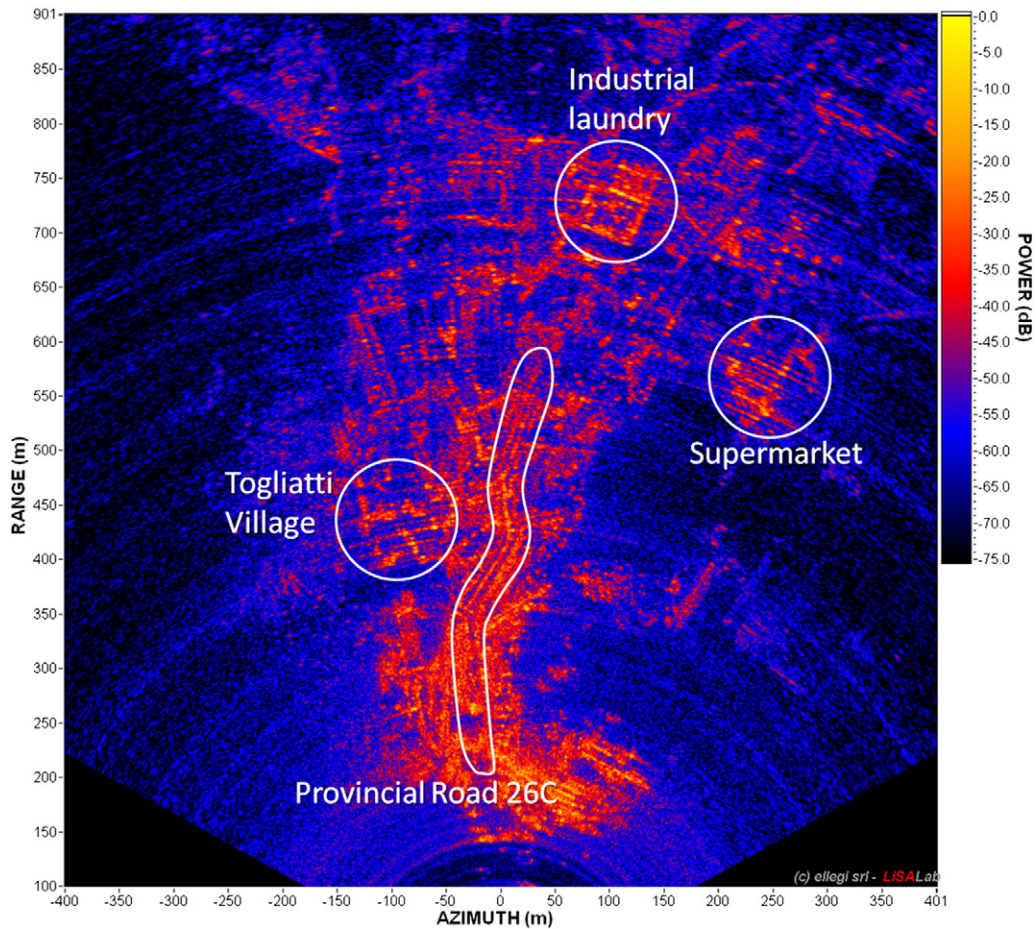
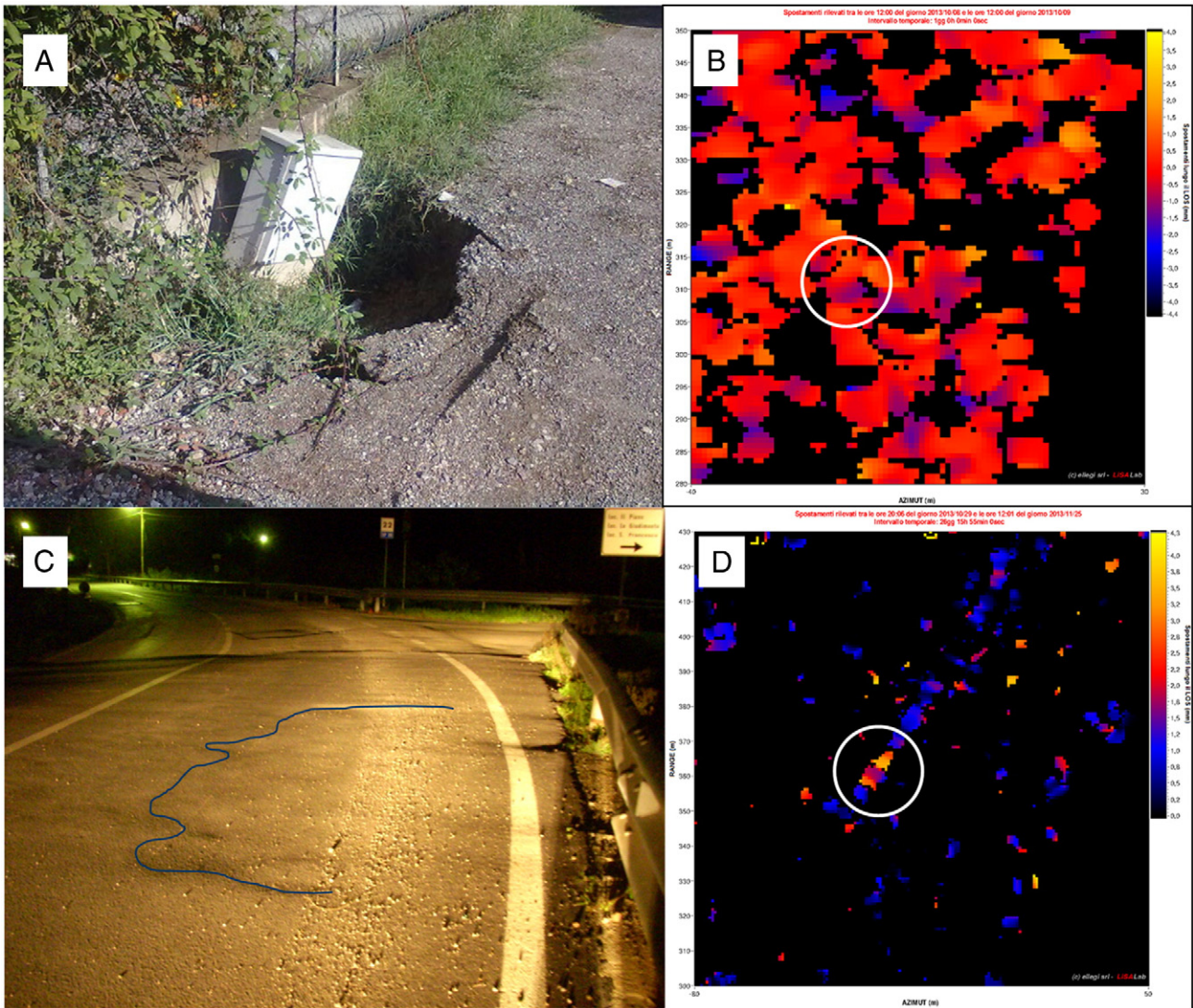


Fig. 4. Power image of the scenario within the GB-InSAR field of view showing the pixels with higher (yellow and red) and lower (blue and black) reflectivity. It is possible to individuate elements of interest represented also in Fig. 1, such as Provincial Road 26C, the Togliatti Village, the supermarket, and the industrial laundry.





**Fig. 5.** Photo of the 09 October 2013 event (A). Its location on a displacement map (spanning from 8 to 9 October 2013) does not show any evidence (B). Photo of the depression ascertained on 25 November 2013 highlighted by the blue line (C) and its location on a displacement map spanning from 29 October to 25 November 2013 (D). The displacement maps are calculated from two daily averaged SAR images (please note that the colour scales of B and D are different).

caused by the small dimensions of the phenomenon and to the presence of a vegetated wall nearby reducing the reflectivity and visibility of the point.

A more successful experience occurred in November 2013 when a 4.5-mm displacement along the LOS (yellow pixels within the circle in Fig. 5D) was recorded along the street in a time period spanning from 29 October to 25 November 2013. This corresponds to around 28.5 mm downward. Other yellow pixels are visible in the surrounding areas; there the coherence is very low owing to the presence of vegetation, therefore these signals are considered as noise. The location of the event is indicated in Fig. 1 as a red point dated 25 November 2013, the day when a field survey confirmed the presence of a lowered area formed in these days (Figs. 1 and 5C). This is where a sinkhole occurred on 31 May 2013. During the survey, the vertical displacement has been roughly evaluated around 25 mm, fitting with the value measured along the GB-InSAR LOS. This deformation did not end up into a fully formed sinkhole. Fig. 5D also shows other clusters of pixels with similar measured displacements but are interpreted as noise because of their smaller dimensions and lower coherence and power values.

Another sector of the same road (located about 80 m west of the previously described one) soon began to attract our attention. The anomaly

was quite evident in long-term interferograms (Fig. 6) and cumulated displacement maps.

On 27 January 2014 an extraordinary monitoring bulletin was dispatched by the Department of Earth Science to the Livorno Province concerning the identified anomaly (see the red dot dated 4 February 2014 in Figs. 1 and 7): ‘from the observation of the displacement maps produced by the GB-InSAR between 29/10/2013 and 26/01/2014, an area showing an anomalous displacement away from the sensor has been detected. This is consistent with a localized ground subsidence, with an accelerating trend during the last week. [...] Due to the dimensions of the interested area and its localization, along the street and near to the events occurred in the past years, a check survey is advisable’.

From 29 October 2013 to 27 January 2014 the movement recorded away from the sensor was 3.3 mm (Fig. 8). A few days later, a centimetric step appeared on the road exactly in the indicated location. Therefore the street was closed, and a subsurface survey was carried out by inserting a probe within a small hole in the tar. This revealed the presence of a large cavity (around 2.5 m wide and 2 m deep; Fig. 7). The hole was immediately filled with boulders, thus ensuring the continuity of monitoring.

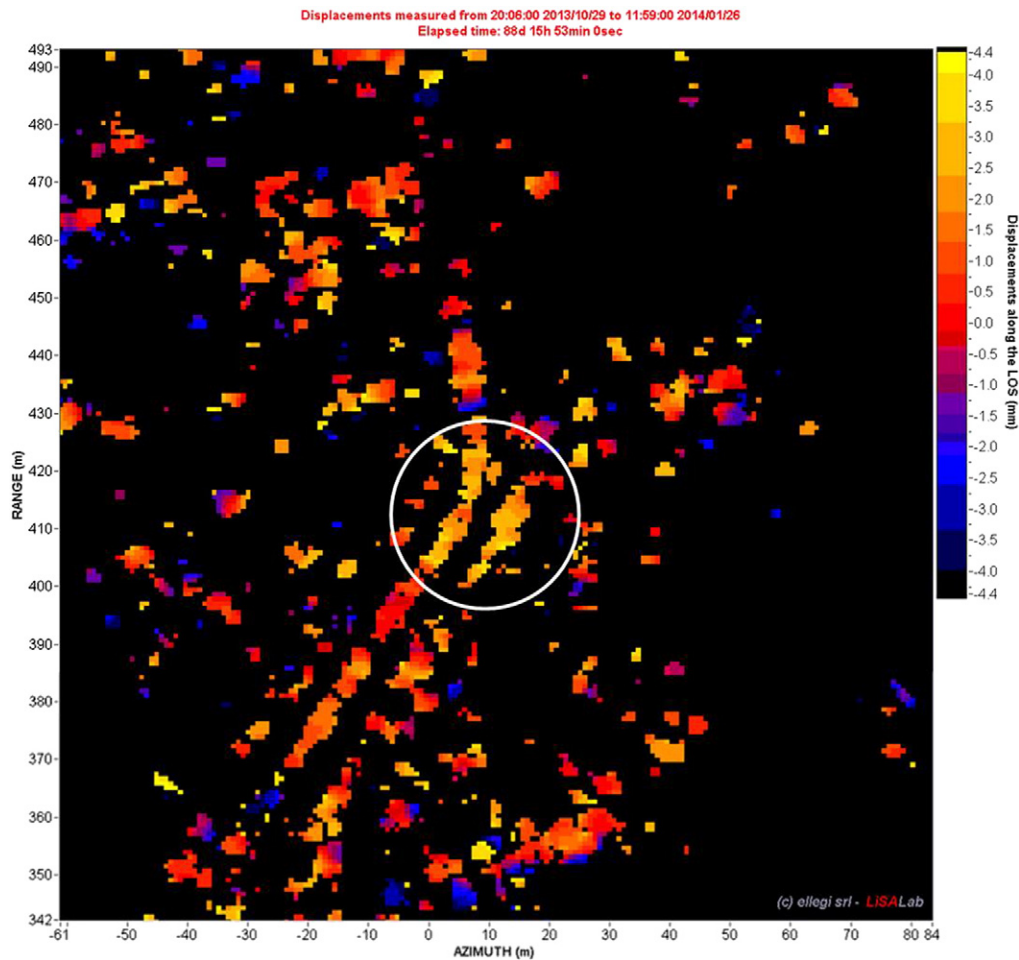


Fig. 6. Long-term interferogram (elapsed time: about 88 days) showing an anomaly along the Provincial Road (white circle).

Once an unstable area is observed, its deformational behaviour can be accurately monitored with time through the automatic extraction of time series. Thus, measured displacements possibly can be compared to some thresholds defined for early warning purposes. Owing to the relatively small dimensions of the phenomenon with respect to the spatial resolution of the displacement maps (Fig. 9), the event is better followed by observing the displacement time series. The time series (blue line) of Fig. 8 has been averaged on 20 pixels in the same area (evidenced in Fig. 9B) in order to reduce the noise. This produces the effect of underestimating the maximum displacements that occurred



Fig. 7. Photo of the cavity below the PR26C detected by the GB-InSAR on 4 February 2014.

(on the cumulated displacement map of Fig. 9 the central pixels of the deforming area record a maximum of 22 mm), but it helps to bring out the general trend. For comparison, the averaged time series of points taken in a stable area in the crops, located at the same range distance as the blue line, is represented (yellow line). The coherence and power intensity values of these latter points are below  $-40$  dB and below 0.7, respectively; on the other hand, on the street reference values are above  $-25$  dB and above 0.9, respectively.

Concerning the blue line, the graph can be divided into three parts: 29 October 2013 to 27 January 2014, 27 January 2014 to 26 February 2014, and 26 February 2014 on. The first period shows a trend of displacement moving away from the sensor; the entity of such movement was enough to allow the detection of an anomaly and therefore to warn the appointed institutions in time. The second period is marked by a strong increase in velocity and a less noisy signal; the deformation is clearly visible on a cumulated displacement map (see Fig. 9 covering almost the same time interval). Eventually the third period is characterized by an increase of the noise and lower displacement velocity comprising essentially stable time intervals (from April to mid June).

A possible trigger for sinkholes in this region is represented by the water pumping operated by the wells that are present in the area and that increment the hydraulic gradient and then favour underground erosive processes. Even though the wells extracting drinking water allegedly do not pump from the superficial aquifer (the one where erosive processes would be stronger), this aquifer is likely interlinked with the one in the karstified limestone, as stated before. Furthermore, the proximity (150 m) of the observed sinkholes to the well field (the second blue dot from the right in Fig. 1) and the temporal nexus between the water pumping interruption and the deceleration in the



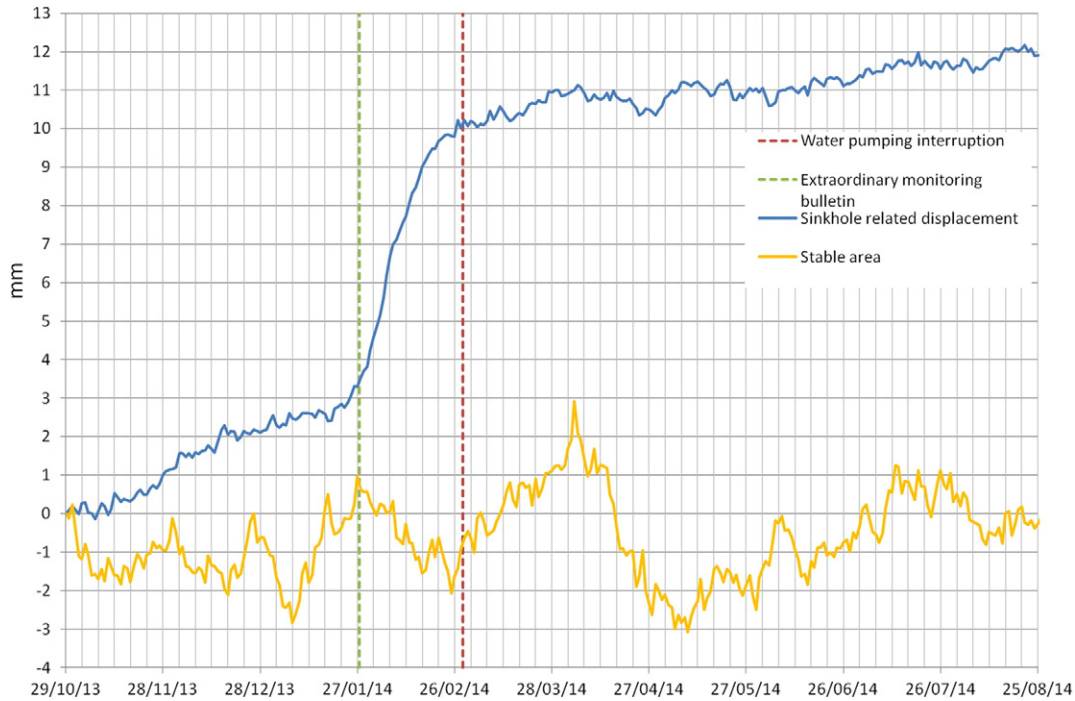


**Fig. 8.** Cumulated displacement time series (blue line) of 20 points within the moving area encircled in Fig. 9B. The values are calculated from daily averaged SAR images. The yellow line shows the averaged displacement of points taken in a stable area in the crops, at the same range distance as the blue line. The green dotted line (27 January 2014 12:46 local time) represents the time when the extraordinary monitoring bulletin was dispatched. The red dotted line (28 February 2014 13:24 local time) indicates the time when the water pumping was interrupted. The displacement is referred to the radar LOS.

measured ground displacement of the 27 January 14 event (Fig. 8) suggest that water extraction may play an important role in sinkhole triggering; however, specific studies should be carried out concerning this issue.

To verify this hypothesis some aerial photos of the area were examined from the Tuscany region database. The detection of past events could prove that even before the presence of the well field, sinkholes occurred. In detail, nine aerial photos relative to the years 1954, 1978, 1988, 1996, 2000, 2005, 2007, 2010 (all at 1:10,000 scale) and 2013 (at 1:2000 scale) have been studied. From the photos, no sinkhole was detected. This could also be owing to the small size of the phenomena with respect to the resolution of the images or to their rapid concealment in populated areas and crops.

## 6. Discussion

Sinkholes typically are catastrophic events that consist of circular chasms propagating upward from natural or anthropic underground cavities. The risk mainly lies precisely in their abrupt nature, which makes them difficult to forecast. The only successes, so far, are thanks to direct observation of cracks in buildings (Buchignani et al., 2008) or, recently, to advanced satellite monitoring (Nof et al., 2013; Jones and Blom, 2014). Even monitoring is difficult; the adopted instruments are derived from other fields and do not perfectly fit some features of this phenomenon, as its small dimensions with respect to the area potentially involved.

For example, satellite interferometry (which shares the same physical principle of GB-InSAR, only on a satellite platform) is a technique commonly used to monitor subsidence (Crosetto et al., 2003; Teatini et al., 2012; Raucoules et al., 2013), landslides (Zebker and Goldstein, 1986; Ferretti et al., 2001; Herrera et al., 2009; Bovenga et al., 2012; Tofani et al., 2013), and sometimes sinkholes (Ferretti et al., 2004; Castañeda et al., 2009; Tessitore et al., 2012; Nof et al., 2013; Jones and Blom, 2014). The main advantages of radar satellite interferometry with respect to sinkhole warning are the possibility to cover large areas,

a good alignment between satellites LOS, the direction of expected movement (vertical), and the availability of historical radar data time series. On the other hand this technique requires high coherence scenarios and therefore a high density of reflectors, which are not always available especially in rural areas. Furthermore, although sometimes sinkhole precursors occurred a few weeks before sinkhole collapses (Nof et al., 2013; Jones and Blom, 2014), the long revisit time of satellites (in the order of days) hinders their use as a means for early warning.

Robotic total stations (RTS) are a possible tool for monitoring and early warning of sinkholes. They are widely used for the monitoring of landslides and structures (Stiros and Psimoulis, 2012; Tsai et al., 2012; Giordan et al., 2013) as they provide precise and accurate position measurements (millimetre level) by measuring distances and angles of specific targets. From this information the complete displacement vector can be exploited. Automatic acquisition at high frequency permits its employment in early warning systems. The main limitation of this technique for sinkhole warning is that all the sinkhole-prone area (or at least the most important elements at risk) should be covered by targets distant from each other no more than the expected diameter of a possible phenomenon.

Global Positioning System (GPS) is able to perform automatic measurements at high acquisition frequency. In certain configurations it can achieve millimetre precision. These features make the GPS a useful instrument in a wide set of applications (Wang et al., 2011; Elnabwy et al., 2013; Zhu et al., 2014); however, its use for sinkhole early warning is severely limited by the cost of displaying a large number of antennas all over the places at risk in the sinkhole-prone area.

Although well-developed sinkholes have already been studied by means of a terrestrial laser scanner (TLS) (Oldow et al., 2008), no cases of TLS used as a prevention tool to detect precursor deformations are reported. This technology permits us to acquire three-dimensional information of the terrain with high accuracy, high resolution (millimetre to centimetre order), and very high data acquisition speeds. Scans acquired in two different times can be compared in order to



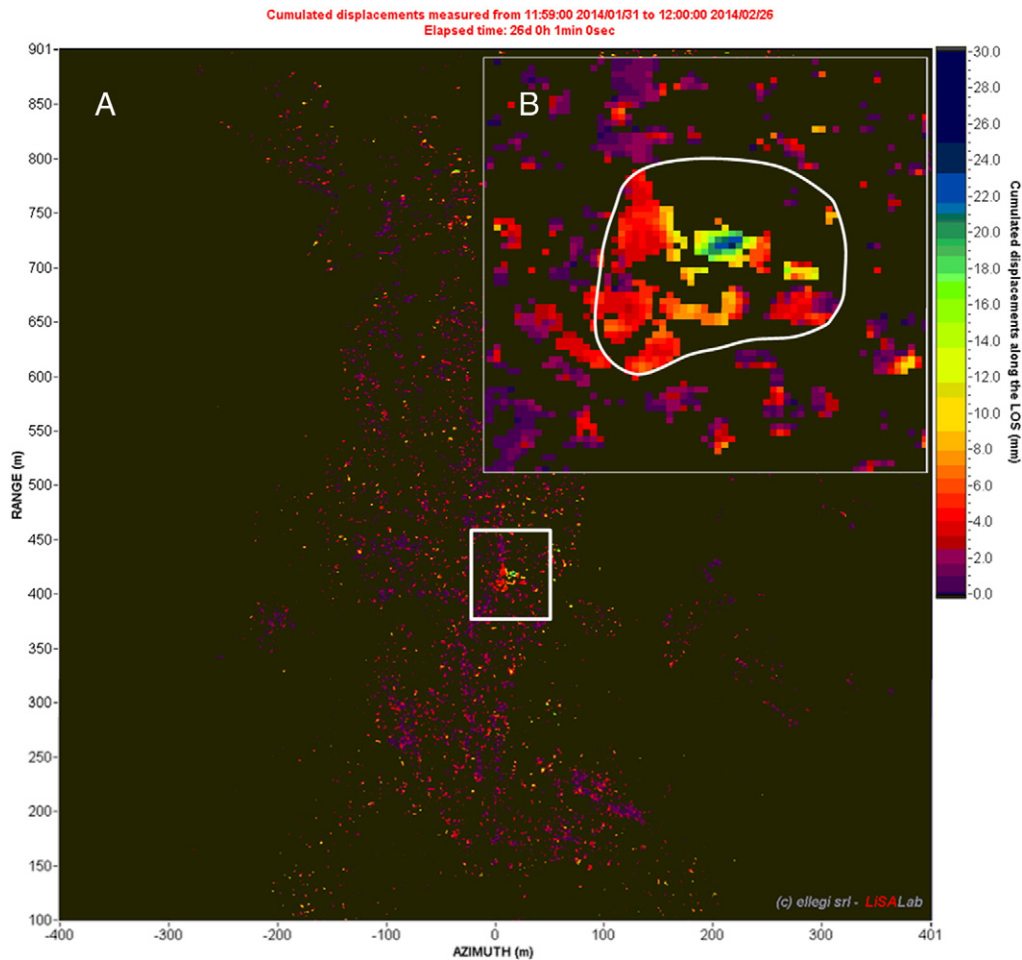


**Fig. 9.** (A) Cumulated displacement map of the period between 31 January 2014 and 26 February 2014 showing a maximum value of 22 mm along the radar LOS within the circled area. (B) Detail of the unstable sector. The white polygon comprehends the 20 points selected for time series extraction (blue line in Fig. 8).

measure the displacement over time, using one of the two as a reference. With respect to RTS and GPS, TLS has the advantage of performing areal monitoring, which does not require the exact knowledge of the location of possible sinkholes. The main limitations are represented by the possible presence of vegetation (like grass) and the need for a high angle between the laser beam and the ground, to preserve precision and accuracy. Furthermore precision of few mm is possible only within a range of a few tens to hundreds of metres (depending on the instrument), which restricts its applicability.

Geophysical methods have been widely applied in the investigation and evaluation of geotechnical problems related to buried sinkholes or epikarstic features since the 1960s (Batayneh et al., 2002). Although seismic reflection and refraction are successfully used to investigate sinkholes, in recent years the most used geophysical technique to identify and localize subsurface cavities has been the ground penetrating radar (GPR) (Carbonel et al., 2014; Kruse, 2014). The GPR allows us to map the shallow subsurface by transmitting short radar pulses into the ground from a surface antenna and by detecting back the reflected wave by a receiving antenna. These methods can be very useful in in situ investigations to evaluate the position and size of sinkholes and to verify the correctness of monitoring data, but they cannot perform any kind of monitoring or early warning themselves.

On the other hand the experimental results displayed above show that sinkhole monitoring and early warning are feasible by using a GB-InSAR apparatus. This is possible because the size of the moving areas is larger than the instrument resolution, and precursor displacements may occur sufficiently long before a catastrophic collapse. In this particular case the high displacement values granted a high

signal-to-noise ratio in the moving area, thus making the monitoring even more proficient.

Data showed plastic deformation lasting for days and proved that the tar of the streets can actually behave like a plastic membrane that exhibits a deformation before experiencing failure, thus allowing adequate monitoring tools to detect it and furnish an early warning. The displacement has been shown to reach values of a few centimetres and to be concentric in nature, with the highest deformation localized in the centre.

In the 27 January 2014 case, the deforming area (around 10 m wide) appeared to be larger than the diameter of the cavity (around 2.5 m) and continued deforming even after the hole was developed and then filled with boulders; this suggests a subsidence zone surrounding the forming sinkhole that implies a general instability phenomenon not only limited to the collapse itself. Similarly, the deformations notified on 25 November 2013 occurred in the same location as a previous sinkhole, although without creating a new one. This can also be interpreted as the settlement of the material used as filling after the collapse.

## 7. Conclusions

A sinkhole-prone area on Elba Island (central Italy) has been experimentally monitored with a GB-InSAR, an apparatus capable of providing displacement maps with high resolution and high precision. The main limit of this application is that the GB-InSAR only measures the component of the movement parallel to its LOS.

In the monitored region nine sinkholes occurred since 2008, all on Provincial Road 26C an important road in Rio Marina municipality or

near it. On 09 October 2013 a 1.5-m-wide sinkhole occurred next to a fence and was not detected by the instrument, not even in back-analysis. This was probably owing to its small dimensions (the average resolution of a pixel here is 1 m × 1 m) and to the covering given by the vegetated wall. This experience is important to provide the detection limits of this application. On 25 November 2013 an area showing 4.5-mm displacement away from the sensor was individuated on the road. Assuming a subsidence movement and projecting the measured value along a vertical downward vector, a total displacement of about 28.5 mm is obtained, consistent with the in situ observations.

On 27 January 2014 a new deforming area was located on the PR 26C. This time a direct probe showed the presence of a 2.5-m-wide cavity almost reaching the street level. This early warning permitted the closure of the road before its catastrophic collapse. The movement continued at least until September 2014 although with lower velocity, thus showing a generalized deformation affecting a 10-m-wide area, centred in the sinkhole.

From this experience the following two major issues in sinkhole monitoring and early warning can be pointed out:

- the small size of a sinkhole with respect to the susceptible area to be monitored;
- the short time between the detection of precursors (if any) and the collapse.

Furthermore, sinkhole study under a civil protection point of view is a subject still needing more research, experiences, and appropriate instruments. Within this framework, this work shows that sinkhole monitoring and early warning are feasible by using a GB-InSAR, typically adopted for landslides. The spatial resolution of the displacement maps allowed us to detect the deforming areas with an advance time sufficient for dispatching a warning and closing the street, probably also thanks to the plastic behaviour of the tar.

## Acknowledgements

The authors are grateful to the Livorno Province that is financing the research (grant number 169/2014-III/13) and in particular to Nicola Gherarducci for his support on the field. Special thanks to the editor Richard Marston, to Guido Luzi, and to three anonymous reviewers for their contribution to earlier versions of the manuscript. The GB-InSAR apparatus used in this application was designed and produced by the Ellegi s.r.l. and based on the proprietary technology GB-InSAR LiSALAB derived from the evolution and improvement of LiSA technology licensed by the Ispra Joint Research Centre of the European Commission.

## References

Atzeni, C., Barla, M., Pieraccini, M., Antolini, F., 2014. Early warning monitoring of natural and engineered slopes with ground-based synthetic-aperture radar. *Rock Mech. Rock. Eng.* 1–12 <http://dx.doi.org/10.1007/s00603-014-0554-4>.

Batayneh, A.T., Abueladas, A.A., Moumani, K.A., 2002. Use of ground-penetrating radar for assessment of potential sinkhole conditions: an example from Ghor al Haditha area, Jordan. *Environ. Geol.* 41 (8), 977–988.

Beck, B.F., Sinclair, W.C., 1986. Sinkholes in Florida: an introduction. Florida Sinkhole Research Institute Report pp. 85–86.

Bezuidenhout, C.A., Enslin, J.F., 1970. Surface subsidence and sinkholes in the dolomitic area of the Far West Rand, Transvaal, Republic of South Africa. *Proc. International Symposium on Land Subsidence, Tokyo, September 1969. International Association of Hydrological Sciences Publication 89*, pp. 482–495.

Bortolotti, V., Fazzuoli, M., Pandeli, E., Principi, G., Babbini, A., Corti, S., 2001. Geology of Central and Eastern Elba Island, Italy. *Ofoliti* 26 (2a), 97–150.

Bovenga, F., Wasowski, J., Nitti, D.O., Nutricato, R., Chiaradia, M.T., 2012. Using COSMO/SkyMed X-band and ENVISAT C-band SAR interferometry for landslides analysis. *Remote Sens. Environ.* 119, 272–285.

Brinkmann, R., Parise, M., Dye, D., 2008. Sinkhole distribution in a rapidly developing urban environment: Hillsborough County, Tampa Bay area, Florida. *Eng. Geol.* 99, 169–184.

Bruno, E., Calcaterra, D., Parise, M., 2008. Development and morphometry of sinkholes in coastal plains of Apulia, southern Italy. Preliminary sinkhole susceptibility assessment. *Eng. Geol.* 99 (3–4), 198–209.

Buchignani, V., Leva, D., Nico, G., Rivolta, C., 2004a. Interferometria Sar da terra per il monitoraggio di un fenomeno di sprofondamento (sinkhole) in Toscana. In: Nisio, S., Panetta, S., Vita, L. (Eds.), *Proc. First Seminary on the State of the Art on Sinkhole Study and the Role of National and Local Administration on Land Management*. APAT, Rome, Italy (In Italian).

Buchignani, V., Lombardi, S., Rizzo, S., Toro, B., 2004b. Il sinkhole di Camaio. In: Nisio, S., Panetta, S., Vita, L. (Eds.), *Proc. First Seminary on the State of the Art on Sinkhole Study and the Role of National and Local Administration on Land Management*. APAT, Rome, Italy, pp. 139–157 (In Italian).

Buchignani, V., Di Filippo, M., Leva, D., Lombardi, S., Rivolta, C., Rizzo, S., Toro, B., 2005. The sinkhole of Camaio (LU-Toscana-Italia). *Geophys. Res. Abstr.* 7, 07915.

Buchignani, V., D'Amato Avanzi, G., Giannecchini, R., Puccinelli, A., 2008. Evaporite Karst and sinkholes: a synthesis on the case of Camaio (Italy). *Environ. Geol.* 53 (5), 1037–1044.

Caramanna, G., Ciotoli, G., Nisio, S., 2008. A review of natural sinkhole phenomena in Italian plain areas. *Nat. Hazards* 45 (2), 145–172.

Carbonel, D., Rodríguez, V., Gutiérrez, F., McCalpin, J.P., Linares, R., Roqué, C., Zarroca, M., Guerrero, J., Sasowsky, I., 2014. Evaluation of trenching, ground penetrating radar (GPR) and electrical resistivity tomography (ERT) for sinkhole characterization. *Earth Surf. Process. Landf.* 39, 214–227.

Castañeda, C., Gutiérrez, F., Manunta, M., Galve, J.P., 2009. DInSAR measurements of ground deformation by sinkholes, mining subsidence, and landslides, Ebro River, Spain. *Earth Surf. Process. Landf.* 34, 1562–1574.

Closson, D., Karaki, N.A., Klinger, Y., Hussein, M.J., 2005. Subsidence and sinkhole hazard assessment in the southern Dead Sea area, Jordan. *Pure Appl. Geophys.* 162, 221–248.

Cramer, H., 1941. Die Systematik der karstdolinen. *Neues Jb. Mineral. Geol. Paläontol.* 85, 293–382 (Abt. B, In German).

Crosetto, M., Castillo, M., Arbiol, R., 2003. Urban subsidence monitoring using radar interferometry: algorithms and validation. *Photogramm. Eng. Remote. Sens.* 69, 775–783.

Del Ventisette, C., Intrieri, E., Luzi, G., Casagli, N., Fanti, R., Leva, D., 2011. Using ground based radar interferometry during emergency: the case of the A3 motorway (Calabria Region, Italy) threatened by a landslide. *Nat. Hazards Earth Syst. Sci.* 11 (9), 2483–2495.

Derbyshire, E., Mellors, T.W., 1988. Geological and geotechnical characteristic of some loess and loessic soil from China and Britain: a comparison. *Eng. Geol.* 25, 135–175.

Di Traglia, F., Del Ventisette, C., Rosi, M., Mugnai, F., Intrieri, E., Moretti, S., Casagli, N., 2013. Ground-based InSAR reveals conduit pressurization pulses at Stromboli volcano. *Terra Nova* 25 (3), 192–198.

Di Traglia, F., Intrieri, E., Nolesini, T., Bardi, F., Del Ventisette, C., Ferrigno, F., Frangioni, S., Frodella, W., Gigli, G., Lotti, A., Stefanelli, C.T., Tanteri, L., Leva, D., Casagli, N., 2014. The ground-based InSAR monitoring system at Stromboli volcano: linking changes in displacement rate and intensity of persistent volcanic activity. *Bull. Volcanol.* 76 (2), 1–18.

Elnabwy, M.T., Kaloop, M.R., Elbeltagi, E., 2013. Talkha steel highway bridge monitoring and movement identification using RTK-GPS technique. *Measurement* 46 (10), 4282–4292.

Faccenna, C., Florindo, F., Funicello, R., Lombardi, S., 1993. Tectonic setting and sinkhole features: case histories from western Central Italy. *Quatern. Proc.* 3, 47–56.

Fairbridge, R.W., 1968. The Encyclopaedia of Geomorphology. In: Reinhold (Ed.), (New York, 1295 pp.).

Ferrelli, L., Guerrieri, L., Nisio, S., Vita, L., Vittori, E., 2004. Relations among seismogenic structures, earthquakes and sinkhole phenomena: a methodological approach in the Apennines (Italy). *Proc. 32nd International Geological Congress, Firenze, Italy, 20–28 August, Volume Abstract, Part 1*, p. 669.

Ferretti, A., Prati, C., Rocca, F., 2001. Permanent scatterers in SAR interferometry. *IEEE Trans. Geosci. Remote Sens.* 39, 8–20.

Ferretti, A., Marco, B., Fabrizio, N., Claudio, P., 2004. Possible utilizzo di dati radar satellitari per individuazione e monitoraggio di fenomeni di sinkholes. In: Nisio, S., Panetta, S., Vita, L. (Eds.), *Proc. First Seminary on the State of the Art on Sinkhole Study and the Role of National and Local Administration on Land Management*. APAT, Rome, Italy, pp. 331–340 (In Italian).

Galve, J.P., Remondo, J., Gutiérrez, F., 2011. Improving sinkhole hazard models incorporating magnitude–frequency relationships and nearest neighbor analysis. *Geomorphology* 134 (1–2), 157–170.

Gigli, G., Intrieri, E., Lombardi, L., Nocentini, M., Frodella, W., Balducci, M., Venanti, L., Casagli, N., 2014. Event scenario analysis for the design of rockslide countermeasures. *J. Mt. Sci.* <http://dx.doi.org/10.1007/s11629-014-3164-4>.

Giordan, D., Allasia, P., Manconi, A., Baldo, M., Santangelo, M., Cardinali, M., Corazza, A., Albanese, V., Lollino, G., Guzzetti, F., 2013. Morphological and kinematic evolution of a large earthflow: the Montaguto landslide, southern Italy. *Geomorphology* 187, 61–79.

Guarino, P.M., Nisio, S., 2012. Anthropogenic sinkholes in the territory of the city of Naples (Southern Italy). *Phys. Chem. Earth* 49, 92–102 (Parts A/B/C).

Gutiérrez, F., Guerrero, J., 2008. A genetic classification of sinkholes illustrated from evaporite paleokarst exposures in Spain. *Environ. Geol.* 53, 993–1006.

Gutiérrez, F., Lucha, P., Guerrero, J., 2004. La dolina de colapso de la casa azul de Calatayud (noviembre de 2003). In: Benito, G., Díez Herrero, A. (Eds.), *Origen, efectos y pronóstico. Riesgos naturales y antrópicos en Geomorfología. VII Reunión Nacional de Geomorfología*, pp. 477–488 (Toledo, In Spanish).

Herrera, G., Fernández-Merodo, J.A., Mulas, J., Pastor, M., Luzi, G., Monserrat, O., 2009. A landslide forecasting model using ground based SAR data: the Portalet case study. *Eng. Geol.* 105 (3–4), 220–230.

Intrieri, E., Gigli, G., Mugnai, F., Fanti, R., Casagli, N., 2012. Design and implementation of a landslide early warning system. *Eng. Geol.* 147–148, 124–136.

Intrieri, E., Di Traglia, F., Del Ventisette, C., Gigli, G., Mugnai, F., Luzi, G., Casagli, N., 2013a. Flank instability of Stromboli volcano (Aeolian Islands, Southern Italy): integration of GB-InSAR and geomorphological observations. *Geomorphology* 201, 60–69.



- Intriери, E., Gigli, G., Casagli, N., Nadim, F., 2013b. Landslide early warning system: toolbox and general concepts. *Nat. Hazards Earth Syst. Sci.* 13, 85–90.
- Jones, C.E., Blom, R.G., 2014. Bayou Corne, Louisiana, sinkhole: precursory deformation measured by radar interferometry. *Geology* 42, 111–114.
- Kaufmann, O., Quinif, Y., 1999. Cover-collapse sinkholes in the Toumais area, southern Belgium. *Eng. Geol.* 52, 15–22.
- Kent, J.D., Dunaway, L., 2013. Real-time GPS network monitors Bayou Corne sinkhole event. *EOS Trans. Am. Geophys. Union* 94 (43), 385–386.
- Krawczyk, C.M., Polom, U., Trabs, S., Dahm, T., 2012. Sinkholes in the city of Hamburg—new urban shear-wave reflection seismic system enables high-resolution imaging of suberosion structures. *J. Appl. Geophys.* 78, 133–143.
- Kruse, S., 2014. Three-dimensional GPR imaging of complex structures in covered karst terrain. In: Lambot, S., Giannopoulos, A., Pajewski, L., André, F., Slob, E., Craeye, C. (Eds.), 15th International Conference on Ground Penetrating Radar GPR 2014. 1, pp. 279–285.
- Lacasse, S., Nadim, F., 2008. Landslide risk assessment and mitigation strategy. In: Sassa, K., Canuti, P. (Eds.), *Landslides – Disaster Risk Reduction*. Springer, Verlag Berlin Heidelberg, pp. 31–61.
- Littlefield, J.R., Culbreth, M.A., Upchurch, S.B., Stewart, M.T., 1984. Relationship of modern sinkhole development to large scale-photolinear features. In: Beck, B.F. (Ed.), *Proc. Sinkholes: Their Geology, Engineering & Environmental Impact*. Balkema, Rotterdam, The Netherlands.
- Luzi, G., Pieraccini, M., Mecatti, D., Noferini, L., Macaluso, G., Tamburini, A., Atzeni, C., 2007. Monitoring of an alpine glacier by means of ground-based SAR interferometry. *Geosci. Remote Sens. Lett.* 4 (3), 495–499.
- Nisio, S., Caramanna, G., Ciotoli, G., 2007. Sinkholes in Italy: first results on the inventory and analysis. *Geol. Soc. Lond., Spec. Publ.* 279, 23–45.
- Nof, R.N., Baer, G., Ziv, A., Raz, E., Atzori, S., Salvi, S., 2013. Sinkhole precursors along the Dead Sea, Israel, revealed by SAR interferometry. *Geology* 41, 1019–1022.
- Oldow, J.S., Alfarhan, M., White, L.S., Ahmed, T., Alvarado, M.I., Cline, J., Shilpakar, P., Aiken, C.L., 2008. Monitoring growth of the Daisetta, Texas sinkhole with terrestrial laser scanning, close range digital photography, and GPS. *Proc. AGU Fall Meeting*, 15–19 December, San Francisco, California, US.
- Paine, J.G., Buckley, S.M., Collins, E.W., Wilson, C.R., 2013. Assessing collapse risk in evaporite sinkhole-prone areas using microgravimetry and radar interferometry. *J. Environ. Eng. Geophys.* 17 (2), 75–87.
- Parise, M., 2012. A present risk from past activities. Sinkhole occurrence above underground quarries. *Carbonates Evaporites* 27 (709–118).
- Pieraccini, M., Tarchi, D., Rudolf, H., Leva, D., Luzi, G., Atzeni, C., 2000. Interferometric radar for remote monitoring building deformations. *Electron. Lett.* 36 (6), 569–570.
- Raucoules, D., Cartannaz, C., Mathieu, F., Midot, D., 2013. Combined use of space-borne SAR interferometric techniques and ground-based measurements on a 0.3 km<sup>2</sup> subsidence phenomenon. *Remote Sens. Environ.* 139, 331–339.
- Rudolf, H., Leva, D., Tarchi, D., Sieber, A.J., 1999. A mobile and versatile SAR system. *Proceedings of Geoscience and Remote Sensing Symposium. IGARSS 1999, Hamburg*, pp. 592–594.
- Salvati, R., Sasowsky, I.D., 2002. Development of collapse sinkholes in areas of groundwater discharge. *J. Hydrol.* 264, 1–11.
- Snyder, S.W., Evans, M.W., Hines, A.C., Compton, J.S., 1989. Seismic expression of solution collapse features from the Florida Platform. *Engineering and Environmental Impacts of Sinkholes and Karst. Proc. of the Third Multidisciplinary Conference on Sinkholes and the Engineering and Environmental Impacts of Karst*, St. Petersburg Beach, Florida, USA, October 2–4.
- Stiros, S.C., Psimoulis, P.A., 2012. Response of a historical short-span railway bridge to passing trains: 3-D deflections and dominant frequencies derived from Robotic Total Station (RTS) measurements Original Research Article. *Eng. Struct.* 45, 362–371.
- Tapete, D., Casagli, N., Luzi, G., Fanti, R., Gigli, G., Leva, D., 2013. Integrating radar and laser-based remote sensing techniques for monitoring structural deformations of archaeological monuments. *J. Archaeol. Sci.* 40 (1), 176–189.
- Tarchi, D., Rudolf, H., Luzi, G., Chiarantini, L., Coppo, P., Sieber, A.J., 1999. SAR interferometry for structural changes detection: a demonstration test on a dam. *Proc. International Geosci. Remote Sens. Symposium. IGARSS, Hamburg Germany*, pp. 1522–1524.
- Tassi, F., Cabassi, J., Rouwet, D., Palozzi, R., Marcelli, M., Quartararo, M., Capecciacci, F., Nocentini, M., Vaselli, O., 2012. Water and dissolved gas geochemistry of the monomictic Paterno sinkhole (central Italy). *J. Limnol.* 71 (2), 245–260.
- Teatini, P., Tosi, L., Strozzi, T., Carbognin, L., Cecconi, G., Rosselli, R., Libardo, S., 2012. Resolving land subsidence within the Venice Lagoon by persistent scatterer SAR interferometry. *Phys. Chem. Earth 40–41 (Parts A/B/C)*, 72–79.
- Tessitore, S., Castiello, G., Fedi, M., Florio, G., Fuschini, V., Ramondini, M., Calcaterra, D., 2012. Integrated monitoring system for ground deformation hazard assessment in Telesse Terme (Benevento province, Italy). *Proc. EGU General Assembly 2012, 22–27 April, Vienna, Austria*, p. 13918.
- Therolf, G., 2005. Sinkholes drive insurance rate increase. Newspaper “St Petersburg Times State” 25th September 2005 (Available at: [http://www.sptimes.com/2005/09/25/Pasco/Sinkholes\\_drive\\_insur.shtml](http://www.sptimes.com/2005/09/25/Pasco/Sinkholes_drive_insur.shtml)).
- Tofani, V., Raspini, F., Catani, F., Casagli, N., 2013. Persistent scatterer interferometry (PSI) technique for landslide characterization and monitoring. *Remote Sens.* 5 (3), 1045–1065.
- Tsai, Z.-X., You, G.J.-Y., Lee, H.-Y., Chiu, Y.-J., 2012. Use of a total station to monitor post-failure sediment yields in landslide sites of the Shihmen reservoir watershed, Taiwan. *Geomorphology* 139–140, 438–451.
- Vallario, A., 2001. *Il dissesto idrogeologico in Campania*. CUEN, Naples, Italy ((Ed.) In Italian).
- Waltham, T., Bell, F., Culshaw, M., 2005. *Sinkholes and Subsidence*. Springer Verlag, Berlin Heidelberg, New York ((Ed.) 382 pp.).
- Wang, J., Peng, X., Xu, C.H., 2011. Coal mining GPS subsidence monitoring technology and its application. *Min. Sci. Technol.* 21 (4), 463–467 (China).
- White, W.B., 1988. *Geomorphology and Hydrology of Karst Terrains*. Oxford University Press, Oxford and New York (Ed.).
- Williams, P., 2003. Dolines. In: Gunn, J. (Ed.), *Encyclopedia of Caves and Karst Science*. Taylor and Francis Group, New York, USA, pp. 304–310.
- Zebker, H.A., Goldstein, R.M., 1986. Mapping from interferometric synthetic aperture radar observations. *J. Geophys. Res.* 91, 4993–4999.
- Zhu, W., Zhang, Q., Ding, X.L., Zhao, C., Yang, C., Qu, F., Qu, W., 2014. Landslide monitoring by combining of CR-InSAR and GPS techniques. *Adv. Space Res.* 53 (3), 430–439.